Acta Crystallographica Section F
Structural Biology and Crystallization Communications
ISSN 1744-3091

Expression, purification, crystallization and preliminary X-ray analysis of an NADP-dependent glyceraldehyde-3-phosphate dehydrogenase from *Helicobacter pylori*

Paul R. Elliott, Daniel Evans, Jacqueline A. Greenwood and Peter C. E. Moody*

Henry Wellcome Laboratories for Structural Biology, Department of Biochemistry, University of Leicester, Leicester LE1 9HN, England

Correspondence e-mail: pcem1@leicester.ac.uk

Received 24 February 2008
Accepted 2 July 2008

The classical glycolytic pathway contains an NAD-dependent glyceraldehyde-3-phosphate dehydrogenase, with NADP-dependent forms reserved for photosynthetic organisms and archaea. Here, the cloning, expression, purification, crystallization and preliminary X-ray analysis of an NADP-dependent glyceraldehyde-3-phosphate dehydrogenase from *Helicobacter pylori* is reported; crystals of the protein were grown both in the presence and the absence of NADP.

1. Introduction

Helicobacter pylori, a micro-aerophilic Gram-negative rod-shaped bacterium, is a dangerous human pathogen that colonizes the upper gastrointestinal tract, resulting in gastritis (Marshall & Warren, 1983). *H. pylori* infection has been implicated in a variety of diseases ranging from peptic ulcers to gastric cancer and mucosal-associated lymphoma (Kuipers *et al.*, 1995; Eidt *et al.*, 1994). Patients infected with *H. pylori* have a 20% lifetime risk of developing peptic ulcer disease and a 2% risk of developing gastric cancer (Ernst, 2000; Kuipers, 1999). *H. pylori* infection is more common in developing countries than in developed countries, with 80% of the population in developing countries carrying the bacteria compared with 25–50% of the population in developed countries (Dunn *et al.*, 1997). Current treatment of *H. pylori* consists of antibiotic treatment coupled with proton-pump inhibitors. Since these treatments have a variety of side effects, and with the onset of antibiotic resistance, new treatments are required (Mendz *et al.*, 1995).

Published analysis of the complete genome of *H. pylori* suggested that its only carbohydrate source is glucose. Furthermore, this analysis suggested that glucose is the main source for substrate-level phosphorylation (Tomb *et al.*, 1997). The *in vitro* growth requirements of the bacteria show that no other carbohydrates are required for growth (Mendz & Hazell, 1993) and the only carbohydrate permease present is glucose-specific (Alm *et al.*, 1999). However, the genes for the key enzymes in glycolysis appear to be absent (Alm *et al.*, 1999; Tomb *et al.*, 1997). The Entner–Doudoroff pathway is an alternative route for glucose catabolism; this pathway is constitutively induced in *H. pylori* (Mendz *et al.*, 1994; Wanken *et al.*, 2003) and has been shown to be the main pathway for the oxidation of glucose (Chalk *et al.*, 1994). Genes for the other carbohydrate metabolic pathways such as the pentose-phosphate shunt and the majority of the gluconeogenic enzymes appear to be present; furthermore, activity has been detected *in vivo* for the pentose-phosphate pathway (Mendz *et al.*, 1993). One common link between all the carbohydrate pathways is glyceraldehyde-3-phosphate. Glyceraldehyde-3-phosphate can feed into the pentose-phosphate shunt for the generation of key five-carbon sugars that are required for DNA biosynthesis. The pentose-phosphate shunt also produces NADPH, which is required for biosynthetic processes and the prevention of oxidative stress. Glyceraldehyde-3-phosphate also acts as a link from the Entner–Doudoroff pathway into glycolysis/gluconeogenesis, whereby glyceraldehyde-3-phosphate undergoes reversible oxidative phosphorylation by glyceraldehyde-3-phosphate dehydrogenase (GAPDH) to

give NADH and 1,3-bisphosphoglycerate. Therefore, an understanding of the pathogen's GAPDH enzyme is crucial to understanding the core metabolism of this organism.

This investigation studied the product of one of the two putative GAPDH genes identified in *H. pylori*, *gapA* (gi:6626253; NCBI, NIH); the gene product from *gapA* is a tetrameteric (4 × 36 kDa) enzyme called GAPDHA. Biochemical analysis, which will be presented elsewhere, is consistent with the dependence of GAPDHA on NADP and raises interesting questions about the function of glucose metabolism in *H. pylori*. GAPDHA has been cloned, expressed, purified and crystallized with and without NADP. Preliminary electron-density analysis was consistent with NADP bound at the active site only when NADP was cocrystallized with GAPDHA.

2. Materials and methods

2.1. Cloning and overexpression

The full nucleotide sequence encoding GAPDHA was cloned into pET151/D (Invitrogen) containing an N-terminal His_6 tag linked by a TEV protease site. The forward primer was CACCATGCCAATTAGAAT and the reverse primer was TATATAGCACAAAATTAA. Dideoxy nucleotide sequencing confirmed the presence of the full-length *gapA* sequence in the vectors.

Escherichia coli strain Rosetta DE3 transformed with pET151/D-gapA was grown at 303 K in the rich medium 2YT supplemented with 100 µg ml^{-1} ampicillin and 35 µg ml^{-1} chloramphenicol. Upon reaching an OD_{600} of 0.6, the culture was cooled to 291 K and incubated overnight at this temperature; isopropyl β-D-1-thiogalactopyranoside induction was not found to be necessary for sufficient overexpression in this case. The cells were harvested the following morning and frozen prior to purification.

2.2. Purification

The purification of His_6-tagged GAPDHA took place as follows. Cell pellets were thawed in buffer *A* (20 m*M* Na_2HPO_4, 500 m*M* NaCl, 50 m*M* imidazole pH 7.4) supplemented with protease-inhibitor cocktail VII (Calbiochem). The suspension was sonicated and cell debris was removed by centrifugation. The supernatant was loaded onto a 5 ml Hi-Trap Nickel Sepharose column (Amersham Biosciences) equilibrated in buffer *A* and eluted against a linear gradient of buffer *B* (20 m*M* Na_2HPO_4, 500 m*M* NaCl, 500 m*M* imidazole pH 7.4). Fractions with enzymatic activity were pooled and dialysed extensively against buffer *C* (20 m*M* Na_2HPO_4, 50 m*M* NaCl, 1 m*M* DTT pH 7.2). To facilitate cleavage of the hexahistidine tag, approximately half of the sample was incubated overnight with TEV protease as stipulated in the manufacturer's instructions (Invitrogen). Samples of cleaved and uncleaved GAPDHA were separately loaded onto a 5 ml Hi-Trap Sulfopropyl Sepharose cation-exchange column equilibrated with buffer *C* and eluted against a linear gradient of buffer *D* (20 m*M* Na_2HPO_4, 1 *M* NaCl, 1 m*M* DTT pH 7.2). A single peak was collected at 550 m*M* NaCl for both the His-tagged and untagged GAPDHA and these were judged to be ∼95% pure by SDS–PAGE analysis. The final yield of protein was approximately 10 mg per litre of culture.

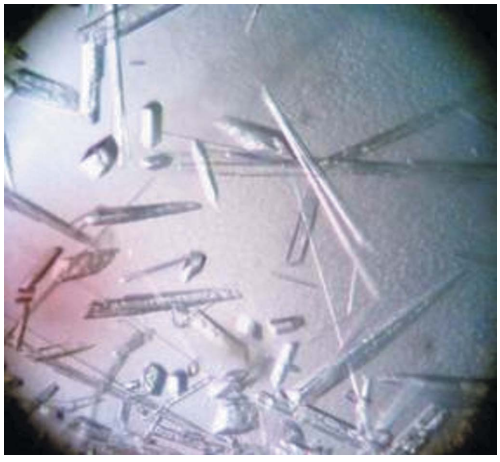

Figure 1
Crystals of untagged apo-GAPDHA grown in 100 m*M* HEPES pH 9.0, 17% PEG 8000. Crystals grew to 200 × 50 µm.

Untagged GAPDHA and His_6-GAPDHA were concentrated to 12 mg ml^{-1} using Amicon Ultra-15 centrifugal filter units (10 kDa molecular-weight cutoff; Millipore) and buffer-exchanged into 20 m*M* MES, 100 m*M* NaCl, 1 m*M* DTT pH 6.5 prior to crystallization.

2.3. Crystallization and data collection

Crystal-growth conditions for untagged GAPDHA were screened by the sitting-drop vapour-diffusion technique using 100 nl drops of protein solution mixed with 100 nl precipitant. The drops were dispensed from a Genomic Solutions Cartesian Honeybee 8+1 (Harvard Bioscience) onto 96-well MRC plates (Innovadyne) with reservoirs containing 80 µl precipitant from the crystal screen kits Wizard I and II and Cryo I and II (Emerald Biosciences) in a humidified chamber (a total of 192 conditions). Plates were sealed with transparent tape and monitored for crystal growth using CrystalProHT (TriTek) plate-storage and imaging systems at 293 and 277 K. Crystallization hits at 293 K were recorded approximately 12 h after the plates were sealed from conditions containing non-ionic precipitants. Refinement of these conditions focused on the higher molecular-weight PEGs (as these appeared to be the most promising) and was performed using a Tecan 75 liquid-handling system (Tecan) and larger crystallization drops dispensed from the Cartesian Honeybee 8+1. The condition that consistently gave reproducible diffraction-quality crystals consisted of 500 nl untagged GAPDHA (12 mg ml^{-1}) mixed with an equal volume of precipitant [100 m*M* HEPES pH 9.0, 17%(*v*/*v*) PEG 8000] equilibrated against a reservoir containing 80 µl precipitant. Crystals grew after one week at 293 K (Fig. 1).

The strategy for exploring crystallization conditions for His_6-GAPDHA (in the presence of 1 m*M* NADP) was the same as described for untagged GAPDHA. Refinement of the initial hit [34%(*v*/*v*) ethanol, 100 m*M* Tris pH 7.2] was performed using a Tecan 75 liquid-handling system (Tecan) to explore the effects of different alcohols and pHs. The final refined condition consisted of 500 nl His_6-GAPDHA (12 mg ml^{-1}) containing 1 m*M* NADP mixed with an equal volume of reservoir comprising 100 m*M* Tris pH 7.3, 36%(*v*/*v*) methanol. Crystals grew after 72 h at 293 K with a clear dependence on the pH of the precipitant (Fig. 2). Attempts to grow crystals of untagged GAPDHA in the presence of NADP were unsuccessful. Similarly, we found no conditions in which crystals of His_6-GAPDHA would grow in the absence of NADP.

Crystals of untagged GAPDHA (Fig. 1) were prepared for cryocrystallography by transferring a single crystal in a litho-loop (Molecular Dimensions) into a final concentration of 15%(*v*/*v*) glycerol in reservoir solution and flash-cooling to 110 K in a stream of boiled-off liquid nitrogen. This method was not successful for His_6-GAPDHA crystals grown using methanol owing to the rapid

Table 1
Summary of data-collection statistics for apo- and holo-GAPDHA.

Values in parentheses are for the highest resolution shell.

	GAPDHA	His_6-GAPDHA + NADP
Wavelength (Å)	0.933	0.934
Space group	$P2_1$	$P3_2$
Unit-cell parameters (Å, °)	a = 75.2, b = 100.6, c = 97.8, α = 90.0, β = 93.7, γ = 90.0	a = 116.9, b = 116.9, c = 95.4, α = 90.0, β = 90.0, γ = 120.0
Resolution limits (Å)	95.4–1.74 (1.82–1.74)	69.5–2.6 (2.74–2.60)
No. of observations	308994 (15449)	158217 (15086)
No. of unique observations	147140 (7357)	43460 (5857)
Completeness	99.0 (99.0)	96.8 (88.3)
$\langle I/\sigma(I)\rangle$	19.0 (2.2)	17.9 (5.7)
R_{merge}†	0.161 (0.534)	0.045 (0.193)

† $R_{merge} = \sum_{hkl}\sum_i |I_i(hkl) - \langle I(hkl)\rangle| / \sum_{hkl}\sum_i I_i(hkl)$, where $I_i(hkl)$ is the intensity of an individual measurement of the reflection with Miller indices hkl and $\langle I(hkl)\rangle$ is the mean intensity of that reflection.

evaporation of methanol upon removal of the plate seal, which caused the crystals to dissolve. This could not be alleviated by harvesting at lower temperatures or attempting to create a methanol-saturated environment. To overcome this problem, various cryoprotectant solutions were injected onto the sitting drops by piercing through the transparent tape with a Hamilton syringe, which allowed efficient harvesting and cryocooling of the crystals prior to data collection. The ability of different cryoprotectants to protect the crystal during the cryocooling process was monitored by obtaining diffraction images of two orientations of the crystal using home-source X-rays and detector (Rigaku RU2HB, Xenocs optics, R-AXIS IV detector). The optimum cryoprotection (as judged by diffraction quality) was afforded by a mixture of 35%(*v*/*v*) 2-methyl-2,4-pentanediol and 100 m*M* Tris pH 7.2.

A complete data set was collected from a single cryocooled crystal of untagged GAPDHA on beamline ID14-2 at the ESRF. An ADSC Q4R CCD detector was used (151.3 mm crystal-to-detector distance) to collect 360 images of 0.5° oscillation at a fixed wavelength of 0.933 Å (a typical image is shown in Fig. 3*a*). Intensities were measured using *MOSFLM* (Leslie, 1992), with the autoindexing routines giving a solution consistent with a primitive monoclinic cell; examination of the principal axes showed an intensity distribution consistent with space group $P2_1$ (statistics are given in Table 1). Solvent-content calculations using four molecules of untagged GAPDHA in the asymmetric unit indicated 50.7% solvent content (V_s) with a Matthews coefficient (V_M) of 2.51 Å^3 Da^{-1} (Matthews, 1968). This is in agreement with all known GAPDH structures, which are also tetramers.

In the case of His_6-GAPDHA (grown in the presence of NADP), diffraction data were collected on beamline ID14-1 at the ESRF with an ADSC Q4R CCD detector (300.7 mm crystal-to-detector distance). 120 images were collected with 0.5° oscillation width at a fixed wavelength of 0.934 Å for a single cryocooled crystal (a typical image is shown in Fig. 3*b*). Analysis using the autoindexing routines of *MOSFLM* suggested a primitive trigonal cell. The data were scaled using *SCALA* (Evans, 2006) in space group *P*3 (statistics are given in Table 1) and examination of the distribution of intensities along the principal axes indicated either a 3_1 or a 3_2 screw axis. Matthews analysis (Matthews, 1968) suggested the presence of a tetramer in the asymmetric unit (V_M = 2.5 Å^3 Da^{-1}; V_s = 50.9% solvent). Molecular replacement using PDB entry 1gd1 (GAPDH from *Bacillus stearo-*

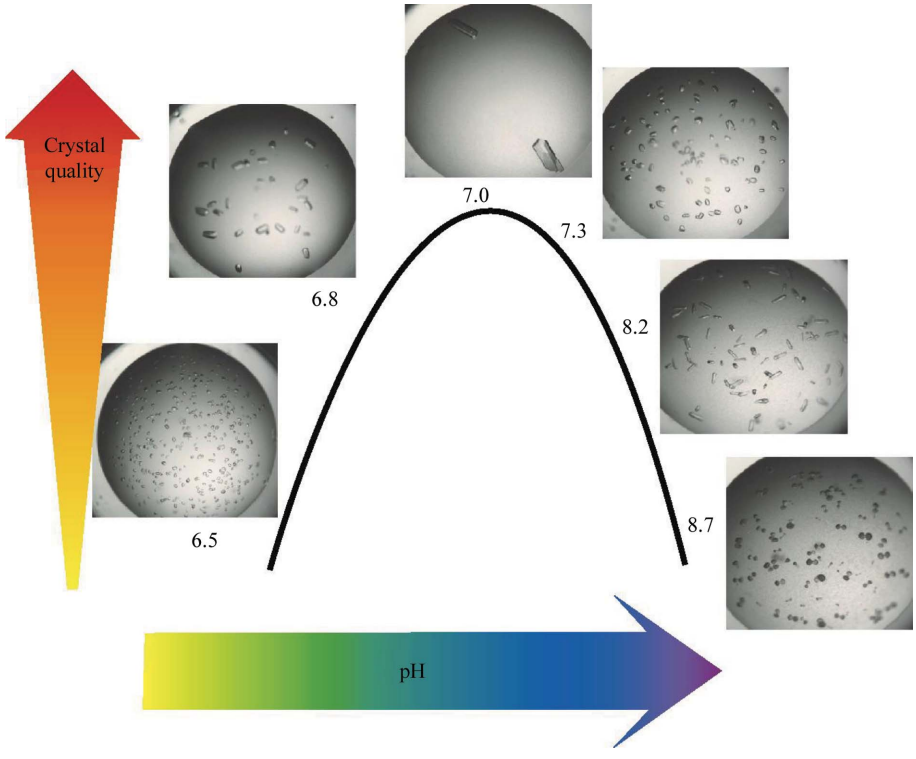

Figure 2
Crystals of His_6-GAPDHA grown in the presence of NADP. It was observed that as the pH increased the quality of the crystals increased until an optimum was reached, after which the quality decreased, with multiple nucleations occurring at the ends of the crystals.

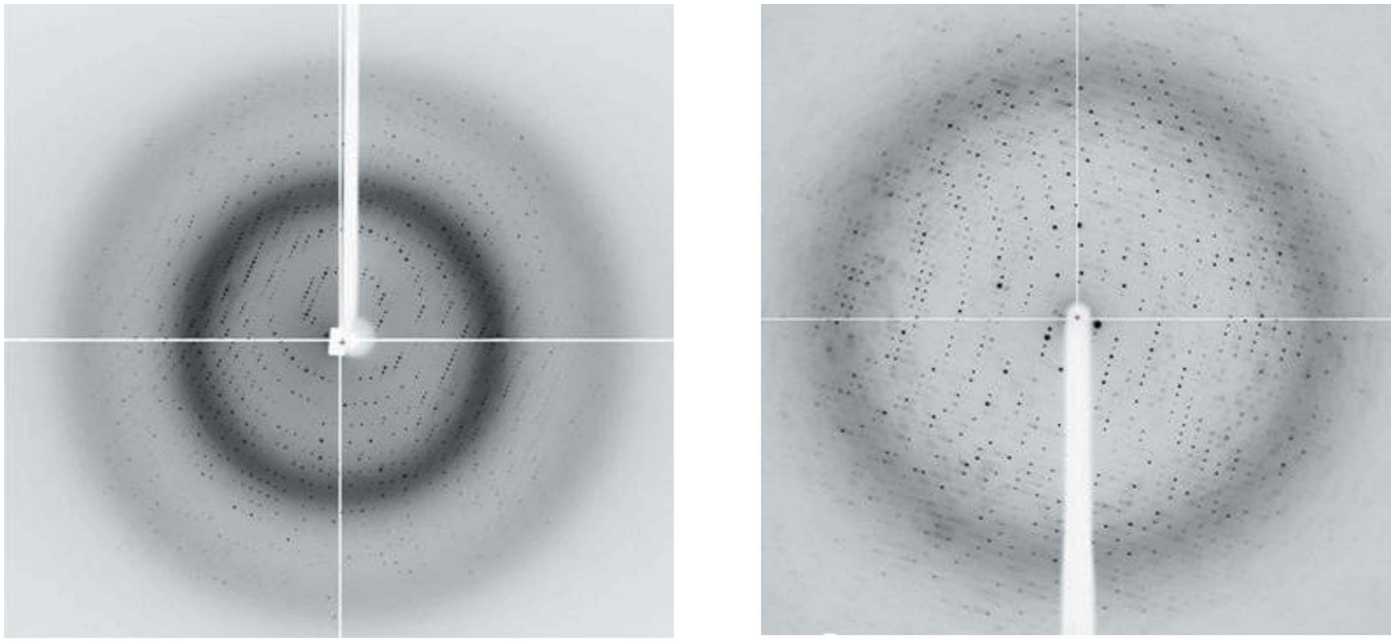

(*a*) (*b*)

Figure 3
(*a*) Typical diffraction pattern for apo-GAPDHA. 360 images were collected with 0.5° oscillation at a fixed wavelength of 0.933 Å. The crystal-to-detector distance was 151.3 mm. (*b*) Typical diffraction pattern of His_6-GAPDHA grown in the presence of NADP. The crystal-to-detector distance was 300.7 mm. 120 images were collected with 0.5° oscillation at a fixed wavelength of 0.934 Å.

thermophilus; Skarzynski *et al.*, 1987) as a search model in *Phaser* (Read, 2001) gave a solution that was only consistent with space group $P3_2$. The sequence identity between the two enzymes is 46%.

3. Results and discussion

GAPDHA has been cloned, expressed and purified. Biochemical studies, which will be presented elsewhere, have shown that GAPDHA is NADP-dependent. Crystals of holo-GAPDHA were obtained when the hexahistidine tag was present and grew using 100 m*M* Tris pH 7.3, 36% methanol as the reservoir buffer. Crystals of apo-GAPDHA only grew when the hexahistidine affinity tag had been removed using TEV protease and belonged to a different space group ($P2_1$) to the holoenzyme ($P3_2$). Preliminary analysis of the electron density derived from the holo-His_6-GAPDHA crystals (which diffracted to 2.6 Å) confirmed the presence of NADP bound to GAPDHA. Work is currently ongoing to obtain a suitable site-directed mutant that is able to form a stable ternary complex with NADP and glyceraldehyde-3-phosphate.

We would like to thank the beamline scientists at ID14-1 and ID14-2 of ESRF. PRE was supported by an MRC studentship.

References

Alm, R. A. *et al.* (1999). *Nature (London)*, **397**, 176–180.
Chalk, P. A., Roberts, A. D. & Blows, W. M. (1994). *Microbiology*, **140**, 2085–2092.
Dunn, B. E., Cohen, H. & Blaser, M. J. (1997). *Clin. Microbiol. Rev.* **10**, 720–741.
Eidt, S., Stolte, M. & Fischer, R. (1994). *J. Clin. Pathol.* **47**, 436–439.
Ernst, P. B. (2000). *Annu. Rev. Microbiol.* **54**, 615–640.
Evans, P. (2006). *Acta Cryst.* D**62**, 72–82.
Kuipers, E. J. (1999). *Aliment. Pharmacol. Ther.* **13**, *Suppl.* 1, 3–11.
Kuipers, E. J., Thijis, J. C. & Festen, H. P. (1995). *Aliment. Pharmacol. Ther.* **9**, *Suppl.* 2, 59–69.
Leslie, A. G. W. (1992). *Jnt CCP4/ESF–EACBM Newsl. Protein Crystallogr.* **26**.
Marshall, B. J. & Warren, J. R. (1983). *Lancet*, **16**, 1311–1315.
Matthews, B. W. (1968). *J. Mol. Biol.* **33**, 491–497.
Mendz, G. L. & Hazell, S. L. (1993). *Arch. Biochem. Biophys.* **300**, 522–525.
Mendz, G. L., Hazell, S. L. & Burns, B. P. (1993). *J. Gen. Microbiol.* **139**, 3023–3028.
Mendz, G. L., Hazell, S. L. & Burns, B. P. (1994). *Arch. Biochem. Biophys.* **312**, 349–356.
Mendz, G. L., Hazell, S. L. & Srinivasan, S. (1995). *Arch. Biochem. Biophys.* **321**, 153–159.
Read, R. J. (2001). *Acta Cryst.* D**57**, 1373–1382.
Skarzynski, T., Moody, P. C. E. & Wonacott, A. J. (1987). *J. Mol. Biol.* **193**, 171–187.
Tomb, J.-F. *et al.* (1997). *Nature (London)*, **388**, 539–547.
Wanken, A. E., Conway, T. & Eaton, K. A. (2003). *Infect. Immun.* **71**, 2920–2923.